ISSN 0208-7774 TRIBOLOGIA 4/2020 p. 17–26
DOI: 10.5604/01.3001.0014.5892

**Mariusz OPAŁKA[*], Piotr KOWALEWSKI[**], Anita PTAK[***]**

# NUMERICAL ANALYSIS OF THE INFLUENCE OF TEMPERATURE ON THE FRICTION RESISTANCE OF A METAL-POLYMER SLIDING PAIR

# NUMERYCZNA ANALIZA WPŁYWU TEMPERATURY NA OPORY TARCIA PARY ŚLIZGOWEJ METAL-POLIMER

**Key words:** FEM, friction, simulation, temperature, bearing, polymers.

**Abstract:** The paper presents numerical calculations of polymer sliding bearings during their operation at low temperatures. Calculations of the frictional moment and the contact area were performed for bearing pans made of PA and PEEK. In the numerical model, the influence of temperature on the mechanical properties (modulus of longitudinal elasticity) and tribological properties (coefficient of friction) were taken into account. The diversified influence of the temperature and thickness of the polymer bearing pans was demonstrated with regards to elements made of different polymer materials. At low temperatures (up to T = -50°C), a different (depending on the used polymer) influence of mechanical and tribological properties on the resistance to motion was found. The ABAQUS calculation package and the finite element method (FEM) were used in the calculations.

**Słowa kluczowe:** MES, tarcie, symulacja, temperatura, łożysko, polimery.

**Streszczenie:** W pracy przedstawiono obliczenia numeryczne polimerowych łożysk ślizgowych podczas pracy w niskiej temperaturze. Obliczenia momentu tarcia oraz powierzchni styku wykonano dla panewek wykonanych z PA i PEEK. W modelu numerycznym uwzględniono wpływ temperatury na własności mechaniczne (moduł sprężystości podłużnej) oraz właściwości tribologiczne (współczynnika tarcia). Wykazano zróżnicowany wpływ temperatury oraz grubości panewki polimerowej dla elementów wykonanych z różnych materiałów polimerowych. W niskiej temperaturze (do $T$ = -50°C) stwierdzono zróżnicowany (w zależności od zastosowanego polimeru) wpływ cech mechanicznych i tribologicznych na opory ruchu. Do obliczeń z zastosowaniem metody elementów skończonych (MES) wykorzystano pakiet ABAQUS do obliczeń.

## INTRODUCTION

Numerous scientific publications have proved that environmental conditions have an influence on the tribological characteristics of a metal-polymer sliding pair. This topic was described quite extensively with regards to temperatures that are higher than the ambient temperature, e.g., in papers **[L. 1–6]**. However, the problem of the friction of sliding polymers at low temperatures has not often been described in the literature. One of the reasons for this discrepancy is the limited availability of equipment that allows experiments to be carried out. Such experiments are quite expensive and the performance of tribological tests is time-consuming. Additionally, there is a problem in ensuring unchanging environmental conditions and in maintaining the repeatability of measurements. This all means that the finite element method is becoming an

[*] ORCID: 0000-0002-0675-9822. Wrocław University of Science and Technology, Faculty of Mechanical Engineering, Department of Fundamentals of Machine Design and Mechatronic Systems, Łukasiewicza 5 Street, 50-370 Wrocław, Poland.
[**] ORCID: 0000-0003-2216-5706. Wrocław University of Science and Technology, Faculty of Mechanical Engineering, Department of Fundamentals of Machine Design and Mechatronic Systems, Łukasiewicza 5 Street, 50-370 Wrocław, Poland.
[***] ORCID: 0000-0002-2177-5812. Wrocław University of Science and Technology, Faculty of Mechanical Engineering, Department of Fundamentals of Machine Design and Mechatronic Systems, Łukasiewicza 5 Street, 50-370 Wrocław, Poland.

increasingly popular method for performing preliminary tests, thanks to which costs can be minimized at the initial stage of research.

The issue of the influence of low temperature on the cooperation of a metal-polymer sliding pair is an important aspect due to the increasing use of polymer sliding systems in machines that operate under changing conditions. The machines and devices that are used in temperate climates are subjected to temperatures reaching even T = -50°C in winter. Literature provides information that ambient temperature changes in the case of thermoplastic polymer materials, by even a few degrees, can significantly affect their mechanical properties **[L. 7–13]**. In turn, the change in mechanical properties translates into changes during the interaction of polymer materials with other materials. Gradt **[L. 14, 15]** reported that, in relation to room temperature, most polymers improve their sliding properties at low temperatures, which is explained by an increase in hardness and mechanical strength. Hübner et al. **[L. 16]** showed that both the friction coefficient and the wear of unmodified materials decrease with a drop in temperature. The author of studies **[L. 17, 18]** also reached similar conclusions. However, the presented research results do not fully explain the phenomena occurring in the cooperating elements. Therefore, in this case, it is extremely helpful to simulate such cooperation using computer calculation techniques.

Computer calculation techniques began to develop in engineering applications over 30 years ago. CAD (Computer Aided Design) and CAE (Computer Aided Engineering) systems are not only used for strength calculations, but are also helpful in tribological issues **[L. 19]**. The flexibility of computer models enables systems with any geometric, material, or load characteristics to be composed. The tribological analysis that is performed using numerical modelling is mainly based on the calculations of the contact problem. Such an issue occurs in places where there is contact between cooperating elements. The physical nature of the contact phenomenon that includes friction is non-linear; therefore, it is difficult to solve using analytical models **[L. 20]**. Due to the fact that there is an increase in the computational capabilities of computers, the contact between cooperating elements is more and more often modelled in engineering calculations. Nearly every point of the mechanical contact between mechanical structures is a friction node. Thanks to computer models, it is possible to determine many parameters that cannot be measured during tests on a physical object, e.g., pressures in the contact zone, or heat flow.

The finite element method (FEM) has been used in engineering calculations since the 1980s. However, for tribological calculations, it has only been widely used since the 1990s **[L. 21–23]**. Kowalewski **[L. 24]** used the finite element method to analyse the pressure distribution in the polymer-metal sliding nodes that are commonly used in tribometers. He showed a significant dependence between the pressure distribution and the stiffness of the polymeric material, as well as between the pressure distribution and its height (distance from the place of support). In turn, Smolnicki, in his monograph **[L. 25]**, modelled large-size rolling nodes.

The processes that occur during the rolling of rolling elements along the bearing raceways with regards to different pairs (a point contact: ball-raceway, and a linear contact: shaft-raceway) were analysed in the paper. Thanks to the use of the finite element method, it was possible to take into account variable parameters such as the adjustment factor or the load. Biernacki **[L. 26]** used the finite element method for inverse analysis. Based on known deformations in the gear pump body, he estimated the value of the coefficient of friction between its elements. Shuoran et al. **[L. 27]** successfully used the finite element method to determine the resistance of various polymer materials to surface fatigue wear after the rolling of a steel element. The results of their simulations are satisfactorily consistent with the experiment.

## MATERIALS AND MEASURING METHODS

The model of the bearing that was adopted for the tests consisted of a polymer pan and a metal shaft. The pan was mounted in a metal frame. The model precisely defined the basic geometric parameters of the pan and the shaft (**Table 1**). The geometric model is shown in **Figure 1**.

**Table 1. Model of the pan and shaft with dimensions**
Tabela 1. Model panewki oraz wałka o następujących wymiarach

| | Shaft | Pan |
|---|---|---|
| Inner diameter $D_w$ [mm] | – | 30.5 |
| Outer diameter $D_z$ [mm] | 30 | 32.5, 33.5, 34.5, 35.5, 36.5, 37.5, 39.5, 41.5 |
| Length $B$ [mm] | 20 | 15 |

The variable parameters in the simulation were as follows: pan thickness $g$ = {1, 1.5, 2, 2.5, 3, 3.5, 4, 5} *mm*, and the operating temperature of a bearing $T$ = {-50, -40, -30, -20, -10, 0, 20}°C. The diameter of the shaft, which is the determinant of the other dimensions of the bearing, was adopted in a way that allows the obtained results to be compared with the results that can be found in other publications **[L. 28]**.

The inner diameter of the pan ($D_n$ – nominal diameter) is 0.5 mm larger than the diameter of the shaft. It falls within the range **[L. 20]**:

$$D_{min} < D_n < D_{max}, \quad (1)$$

where

$$D_{min} = \sqrt{\frac{\pi F_N}{2\lambda p_{dop}}} \quad (2)$$

$D_{min}$ was determined from the condition of permissible pressures for the material of the pan.

$$D_{max} = X_T \frac{\left(2\lambda^2 + \frac{350}{3}\right)60\,000}{\pi n} e^{\frac{1}{H-1}} \quad (3)$$

where
$F_N$ – normal load of the bearing [N]
$\lambda$ – dimensional factor [-] ($\lambda = B/D_w$; where $B$ – the pan's length, $D_w$ – the inner diameter of the pan)
$p_{dop}$ – permissible pressure for the material of the pan [MPa]
$XT$ – temperature coefficient [-]
$n$ – rotation speed [1/min]
$H$ – correction factor, which takes into account the type of movement in the bearing [-]

Afterwards, for the adopted nominal diameter, the following outer diameter $D_z$ was determined using the following formula **[L. 20]**:

$$D_z = -0.0001D_n^2 + 0.087D_n + 1.14 \quad (4)$$

The outer diameter of the polymer bearing pan that was determined using the above Formula (4) is equal to $D_z$ = 37.9 mm. For this reason, it was decided to adopt the dimensions of the pan presented above. In turn, the selection of the temperatures results from the fact, as mentioned in the introduction, that no structural changes occur in plastics, such as the tested thermoplastic polymers, below the temperature $T$ = -50°C. This ensures the continuity of the tribological processes. Moreover, machines and mechanical devices operating in a moderate climate are not exposed to temperatures lower than $T$ = -50°C.

The plastics that were used for the analysis of the pan's material were Polyamide (PA6) and polyetheretherketone (PEEK). The choice of the above-mentioned polymer materials was dictated by the fact that they are commonly used in sliding elements of machines, they have good tribological properties, and above all, they can work in a wide temperature range (from $T$ = -50°C to $T$ = +100°C for PA6, and from $T$ = -60°C to $T$ = + 310°C for PEEK).

For the purpose of the numerical calculations, some simplifications were adopted. They were necessary in order to perform the full simulation. These mainly involve the quasi-static operating conditions, the adoption of the ideal geometry of the elements (the omitting of shape deviations), and the operation in thermal equilibrium conditions and stable friction conditions (constant sliding speed, pressure, temperature). Due to the fact that polymers are characterized by viscoelastic properties (which are also dependent on temperature), which necessitates the use of nonlinear material models and the performing of dynamic calculations, simplifications that assume the elastic behaviour of materials were also adopted. This is only possible within the range of small deformations, and this occurs in the case of the discussed simulation.

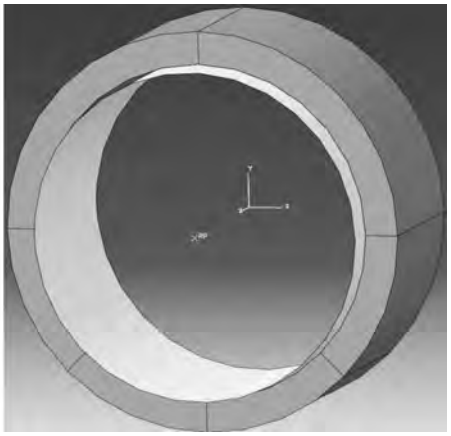

**Fig. 1. 3D Model of the tested object (shaft, bearing, pan)**
Rys. 1. Model 3D badanego elementu (wał, miska, łożyska)

The model adopted for the calculations consisted of a hollow shaft, which is the bearing pan, and a cylindrical surface, which is the shaft. First of all, the material characteristics of the pan were assigned (**Table 2**), then the contact interactions were implemented (surface-to-surface), and finally the characteristics of the contact between the steel shaft and the polymer pan were also assigned. In the next step of preparing the simulation, appropriate restraints and loads were applied onto the objects. The pan was fixed on the outer surface, and all of its (6) degrees of freedom (3 translations and 3 rotations) were omitted. In turn, the shaft was rigidly connected to the reference point (RP in **Fig. 1**). The shaft loads were controlled by applying appropriate forces/moments/restraints/excitations to the reference point. Throughout the simulation, the shaft was translationally restrained in the $Z$ and $X$ axes, and rotationally restrained in the $Y$ and $X$ axes.

Two calculation steps were used:

1. The shaft was loaded with a radial force of $F$ = 150 N ($F$ = -150 N in the $Y$ axis). The low value of the unit pressure results from the fact that there is a possibility of an increase in the local pressure due to the increase in material stiffness. This is caused by the temperature drops.
2. The rotation of the shaft by α = 0.05 rad = 2.8° (α = 0.05 rad in the Z axis) – kinematic excitation. The use of kinematic excitation, i.e. by the application of the displacement, allows the convergence of equations in the simulation to be quickly found.

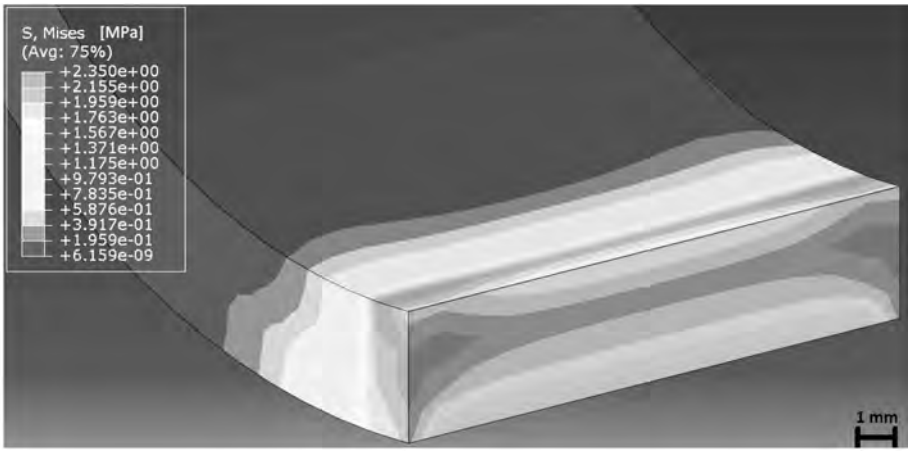


**Fig. 2. Distribution of reduced stress according to the Huber-Misses hypothesis in the pan material (PA6, $T$ = - 50°C, $g$ = 3 mm). Visible stress concentration area under the material surface (Bjelajew point). The stress does not exceed that allowable for the material**

Rys. 2. Rozkład naprężeń zredukowanych wg Hipotezy Hubera-Miessesa w materiale panewki (PA6, $T$ = -50°C, $g$ = 3 mm). Widoczne miejsce koncentracji naprężeń pod powierzchnią materiału (punkt Bjelajewa). Naprężenia nie przekraczają dopuszczalnych dla materiału

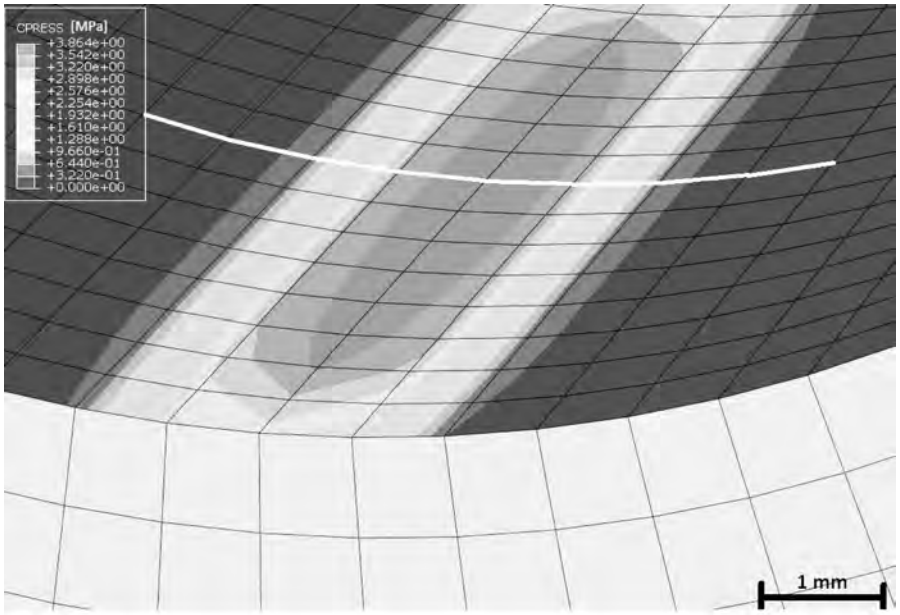


**Fig. 3. Distribution of the contact pressures in the polymer material (PEEK, $T$ = -30°C, $g$ = 3 mm). The white thick line indicates the path along which the stress values for the diagrams were read**

Rys. 3. Rozkład nacisków stykowych w materiale polimerowym (PEEK, $T$ = -30°C, $g$ = 3 mm). Linią białą grubą zaznaczono ścieżkę (path), wzdłuż której odczytywano wartości naprężeń do wykresów

Forcing the displacements by applying a force or a moment of force leads to computational instability (because the force of the static friction is greater than the force of the kinetic friction).

The calculated values were the following: the contact area between the shaft and the pan, the reduced stresses according to the Huber hypothesis (**Fig. 2**), the distribution pressure on the surface of the pan (**Fig. 3**), and the frictional moment (**Fig. 4** and **Fig. 5**). The results obtained in this way represent the resistance to motion during the first few revolutions of the shaft.

The model uses volumetric elements (C3D8S) – 8 Brick type nodal linear elements with an improved visualization of surface stresses for the modelling of the pan and surface elements (R3D4) – four-node rigid elements for the modelling of the shaft. This simplification was chosen for two reasons:

1. The difference in the longitudinal elasticity coefficients of steel ($E \approx 200000$ MPa) and the modelled polymers ($E \approx 2000$ MPa for PA6 and $E \approx 4000$ MPa for PEEK) is so large that steel elements are commonly assumed to be infinitely rigid **[L. 24, 29]** (steel approx. 50–100 times stiffer).
2. The use of surface elements in order to reflect the shape of the shaft allows their number (in relation to the number of volumetric elements) to be reduced. This shortens the simulation time by 72% ($t$ = 241 s solid – $t$ = 68 s rigid; after optimization $t$ = 213 s solid – $t$ = 58 s rigid).

Such a simplification is used in the literature when modelling metal-polymer frictional contacts **[L. 28, 30]**.

**Table 2. Mechanical properties of the PA6 and PEEK used in the analysis [L. 11, 31]**
Tabela 2. Właściwości mechaniczne PA6 oraz PEEK użyte w symulacji **[L. 11, 31]**

| | Temperature $T$ [°C] | Value of the coefficient of friction μ | | | E [MPa] | $\nu$ |
|---|---|---|---|---|---|---|
| | | Pressure $p$ [MPa] | | | | |
| | | 0.5 | 1 | 3 | | |
| PA6 | 20 | 0.249 | 0.259 | 0.427 | 1982 | 0.35 |
| | 0 | 0.24 | 0.305 | 0.39 | 3301 | |
| | -10 | 0.298 | 0.379 | 0.421 | 3759 | |
| | -20 | 0.314 | 0.314 | 0.4 | 4082 | |
| | -30 | 0.332 | 0.346 | 0.323 | 4270 | |
| | -40 | 0.335 | 0.354 | 0.316 | 4324 | |
| | -50 | 0.271 | 0.289 | 0.276 | 4243 | |
| PEEK | 20 | 0.395 | 0.366 | 0.411 | 3700 | 0.4 |
| | 0 | 0.344 | 0.281 | 0.365 | 4484 | |
| | -10 | 0.416 | 0.35 | 0.337 | 4547 | |
| | -20 | 0.427 | 0.324 | 0.371 | 4485 | |
| | -30 | 0.403 | 0.3 | 0.33 | 4369 | |
| | -40 | 0.379 | 0.328 | 0.336 | 4269 | |
| | -50 | 0.328 | 0.281 | 0.333 | 4256 | |

## RESULTS

Based on the conducted simulations, the moments of friction of the modelled bearings with different pan thicknesses during their operation at different temperatures were determined. The values of the moment of friction for individual material contacts are presented in **Table 3** and **Table 4**, as well as in **Fig. 4** and **Fig. 5**.

As can be seen, the course of changes in the moment of friction in the analysed bearings is different. In both cases, there are significant fluctuations in the value of the resistance to motion in the tested temperature range. However, there is a general tendency for the moment of friction to increase with an increase in operating temperature. In the case of the pan made of PA6, the increase occurs within the range from $T$ = -50°C to $T$ = -10°C. For PEEK, this increase, except for local changes ($T$ = -10°C), occurs in the entire range of the tested temperatures.

Changes in the resistance to motion related to the thickness of the polymer pan also do not show a clear trend. In the case of the bearing with the pan made of PA6, the thickness of the sliding element clearly affects the moment of friction within a positive temperature range. For the bearing made of PEEK, the values of the moment of friction are similar for all the thicknesses of the pan, except for $g$ = 5 mm. In this case, the frictional resistance is the lowest.

In order to demonstrate the influence of the mechanical and tribological properties on the phenomena of friction in the tested bearings, and thus on the resistance to motion, the contact area and pressure distributions during the operation of the bearings at different temperatures were also determined. Exemplary distributions of these quantities with regards to the temperature and thickness of the pan are shown in **Fig. 7** and **Fig. 8** for the PA6, and in **Fig. 9** and **Fig. 10** for the PEEK.

**Table 3. Determined values of the moment of friction for PA6**
Tabela 3. Wyznaczony moment tarcia dla PA6

| **PA6** | | | | | | | | |
|---|---|---|---|---|---|---|---|---|
| **Temperature $T$ [°C]** | **Pan thickness $g$ [mm]** | | | | | | | |
| | 1 | 1.5 | 2 | 2.5 | 3 | 3.5 | 4 | 5 |
| 20 | 926.27 | 884.90 | 864.77 | 850.63 | 840.61 | 835.17 | 820.65 | 809.54 |
| 0 | 881.37 | 867.58 | 848.94 | 843.58 | 841.04 | 838.03 | 835.86 | 830.77 |
| -10 | 952.89 | 951.99 | 937.15 | 927.69 | 926.94 | 927.29 | 926.75 | 927.46 |
| -20 | 904.00 | 904.00 | 899.14 | 889.55 | 883.68 | 879.21 | 875.43 | 860.24 |
| -30 | 732.34 | 731.53 | 731.50 | 732.30 | 733.03 | 733.90 | 734.77 | 741.60 |
| -40 | 716.88 | 715.92 | 715.82 | 717.66 | 719.05 | 720.57 | 721.95 | 732.73 |
| -50 | 625.52 | 625.02 | 624.86 | 624.43 | 624.42 | 624.81 | 625.43 | 630.85 |

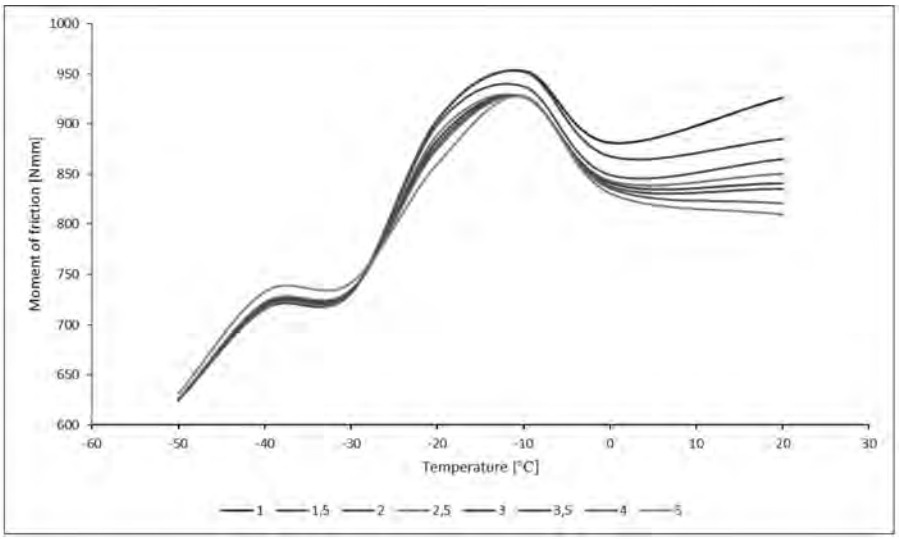


**Fig. 4. Diagram of changes in the moment of friction with regards to temperature for PA6 pans of different thickness**
Rys. 4. Wykres zmian momentu tarcia względem temperatury dla panewek z PA6 o różnej grubości

**Table 4. Determined values of the moment of friction for PEEK**
Tabela 4. Wyznaczony moment tarcia dla PEEK

| PEEK | | | | | | | | |
|---|---|---|---|---|---|---|---|---|
| **Temperature *T* [°C]** | **Pan thickness *g* [mm]** | | | | | | | |
| | 1 | 1.5 | 2 | 2.5 | 3 | 3.5 | 4 | 5 |
| 20 | 930.23 | 929.36 | 928.10 | 925.01 | 921.50 | 917.47 | 914.54 | 905.56 |
| 0 | 824.20 | 823.89 | 823.74 | 822.61 | 820.89 | 818.98 | 816.80 | 788.72 |
| -10 | 764.22 | 763.45 | 763.28 | 764.17 | 768.31 | 771.79 | 773.50 | 769.84 |
| -20 | 839.20 | 838.61 | 838.42 | 839.22 | 841.98 | 843.77 | 843.45 | 820.12 |
| -30 | 746.72 | 746.30 | 746.19 | 748.94 | 752.93 | 755.16 | 755.09 | 734.85 |
| -40 | 761.17 | 760.56 | 760.41 | 762.83 | 765.15 | 766.09 | 765.91 | 757.42 |
| -50 | 752.71 | 752.45 | 752.35 | 751.51 | 750.84 | 749.19 | 747.39 | 729.52 |

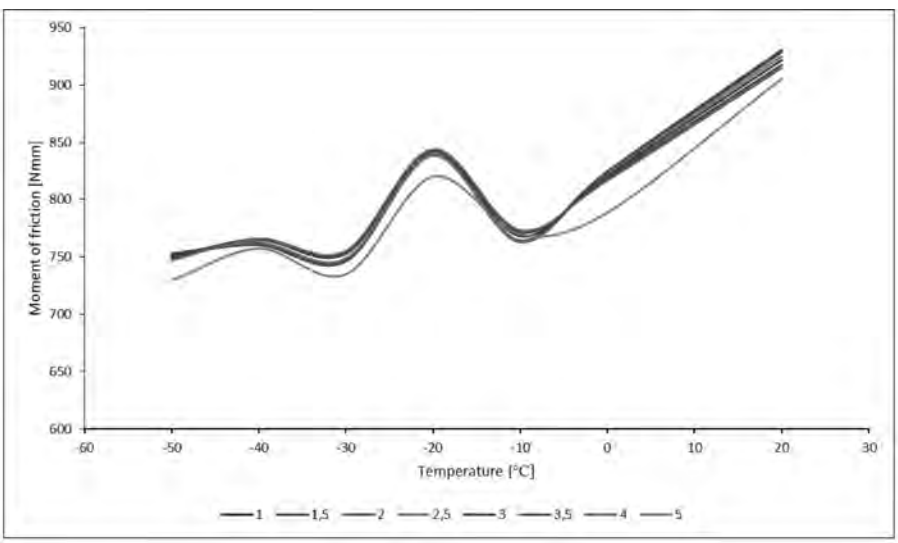


**Fig. 5. Diagram of changes in the moment of friction with regards to temperature for PEEK pans of different thickness**
Rys. 5. Wykres zmian momentu tarcia względem temperatury dla panewek z PEEK o różnej grubości

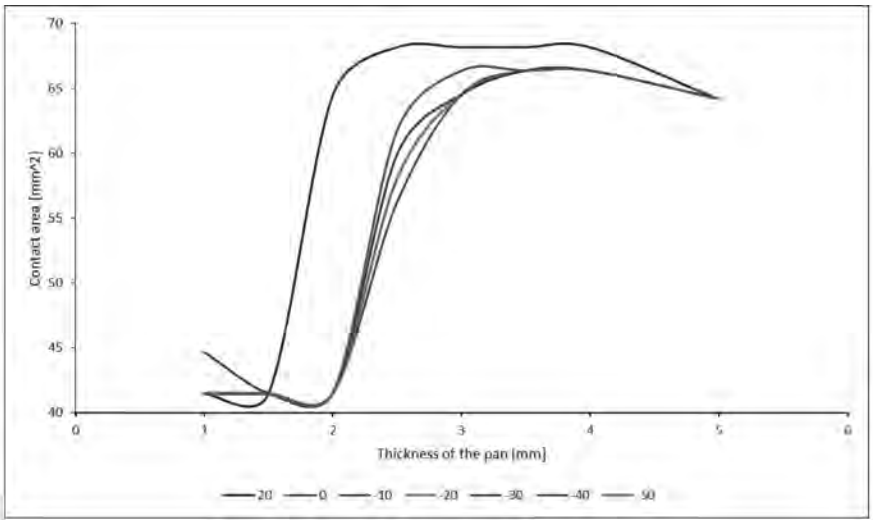


**Fig. 6. The relations between the contact area and the thickness of the pan for different bearing operating temperatures for PEEK**

Rys. 6. Zależność między powierzchnią kontaktu i grubością panewki dla różnej temperatury pracy łożyska dla PEEK

## DISCUSSION

The conducted simulations showed the significant influence of the bearing operating temperature on the occurring moment of friction. In the studied temperature range ($T$ = -50°C to $T$ = 20°C), the differences in the values of the moment of friction for PA6 reached up to ⅓ of its value. There is a tendency for an increase in the resistance to motion with an increase in the temperature. However, there are also local deviations from this tendency.

When analysing the influence of individual design parameters on the moment of friction, the influence of the thickness of the polymer pan can also be noticed. Significant changes in pressure distributions for pans of different thicknesses can especially be noticed in the case of the PEEK pan (**Fig. 7**). The thinner the pan, the more concentrated the contact area is. Nevertheless, when analysing the input data of the dependence between the coefficient of friction and the unit pressure, it can be stated that the amount of pressure has a smaller impact on the resistance to motion than the changes in temperatures. It can therefore be concluded, from a tribological point of view, that the thickness of the pan is not an important design parameter for this material.

In the case of pans made of PA6, the influence of the thickness of the pan only becomes important at positive temperatures. The pressures for thick pans ($g$ = 3 mm and $g$ = 5 mm) are lower than those for thin ones ($g$ = 1 mm), and the contact area also increases (**Fig. 3**). Because of the fact that the influence of the unit pressure on the coefficient of friction is large in the case of PA6 (**Table 2**), there is an increase in the moment of friction (**Fig. 4**). Interestingly, for PEEK, for which the contact area also increases at positive temperatures (**Fig. 3**), the effect involves an increase in the moment of friction (**Fig. 5**). This is due to the not so large influence of the unit pressure on the value of the coefficient of friction (**Table 3**).

Summing up, it can be stated that tribological properties (characteristics $\mu = f(p)$) or mechanical properties, depending on the plastic material, can have a decisive influence on the value of a bearing's resistance. This is also confirmed by the research described in **[L. 32]**.

## CONCLUSION

After comparing the simulation results with the data, it cannot be clearly stated that any of the factors are of decisive importance. Resistance to motion in the modelled polymer bearings depends on both changes in the tribological and mechanical properties, as well as on the operating temperature.

The thickness and elasticity of the pan (which depend on the temperature) directly affect the size of the contact area and the pressure distribution in the node of friction. If the value of the coefficient of friction is strongly dependent on the unit pressure, the tribological properties will dominate and affect the value of the moment of friction (PA6). If the tribological characteristics ($\mu = f(p)$) are of a stable nature, then the influence of the mechanics of the plastic on the size of the contact area and, consequently, on the value of the moment of friction will be the dominant one.

The possibilities and usefulness of numerical methods in calculating the resistance to motion of

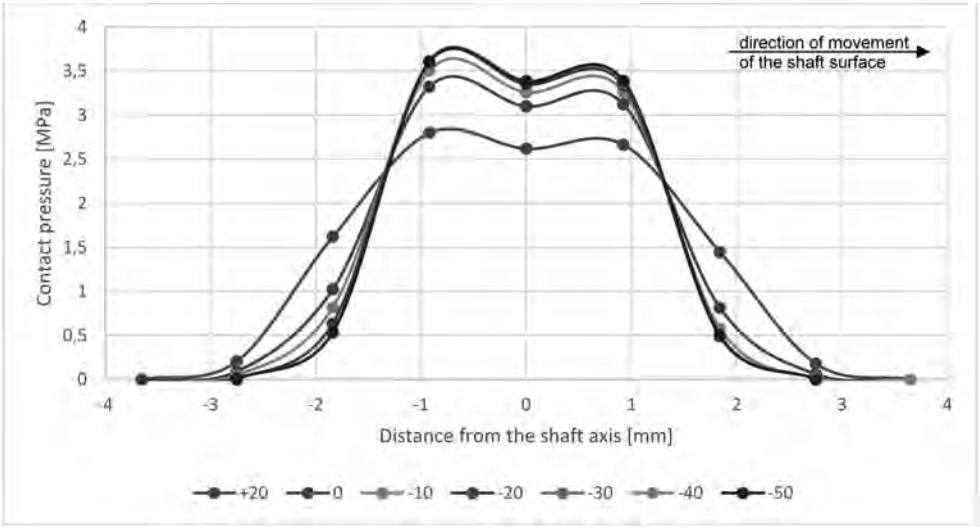


**Fig. 7. Distribution of the contact pressure between the shaft and the pan made of PA6 when the thickness of the pan $g$ = 3 mm at different operating temperatures T**

Rys. 7. Rozkład nacisku między wałem a panewką dla PA6 przy grubości panewki $g$ = 3 mm dla różnych temperatur

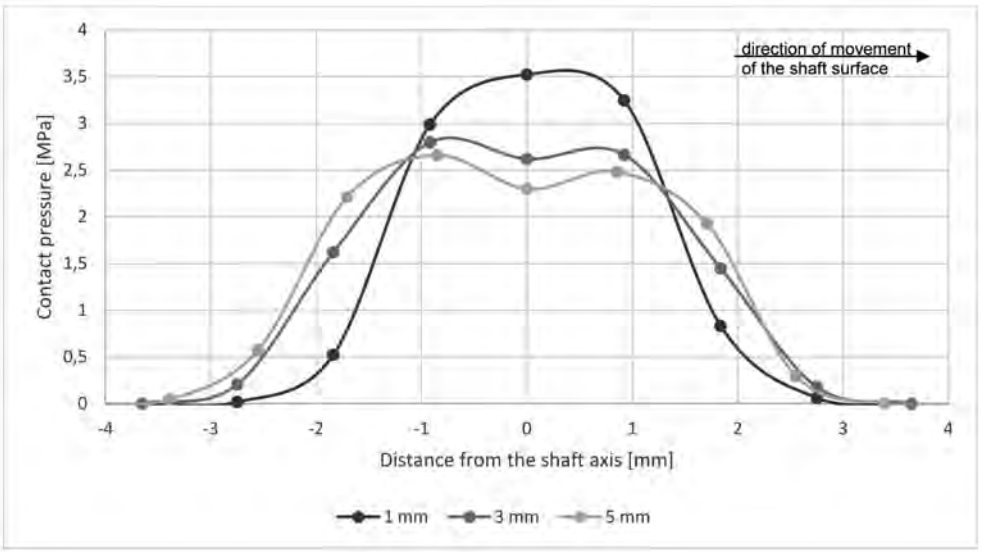


**Fig. 8. Distribution of the contact pressure between the shaft and the pan for PA6 at $T$ = 20°C for different thicknesses of the pan**

Rys. 8. Rozkład nacisków stykowych między wałem a panewką dla PA6 w temperaturze $T$ = -20°C dla różnych grubości panewki

sliding elements should be emphasized. These methods are particularly applicable in the case of materials with complex mechanical characteristics, such as plastics. FEM analysis allows changes in the moment of friction with regards to the design parameters and environmental conditions to be determined. The presented example can be used as a guideline for the design of polymer bearings and other bearing systems. However, it should be emphasized that the preparation of this type of simulation requires basic tribological and mechanical characteristics, and also a lot of experience.

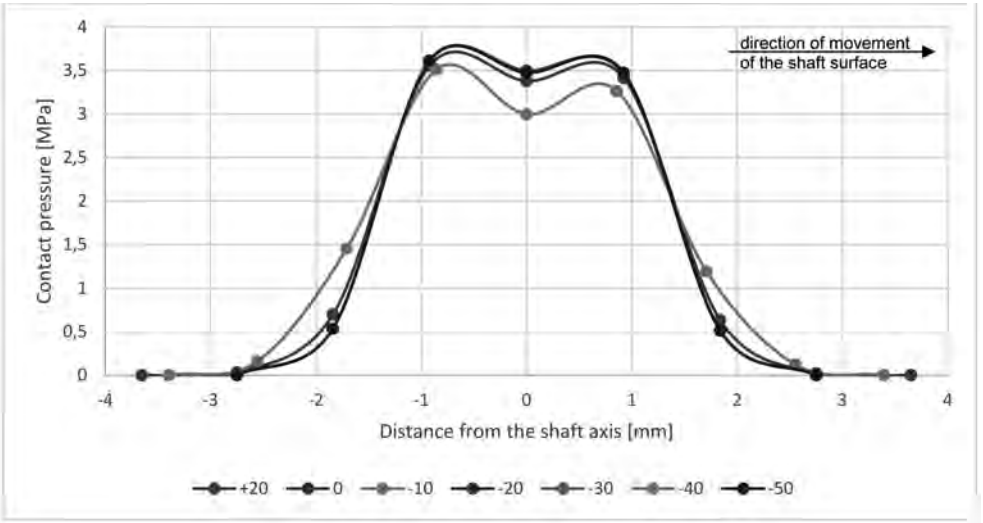


**Fig. 9. Distribution of the contact pressure between the shaft and the pan made of PEEK when the thickness of the pan $g$ = 3 mm at different operating temperatures $T$**

Rys. 9. Rozkład nacisku między wałem a panewką dla PEEK przy grubości panewki $g$ = 3 mm dla różnych temperatur

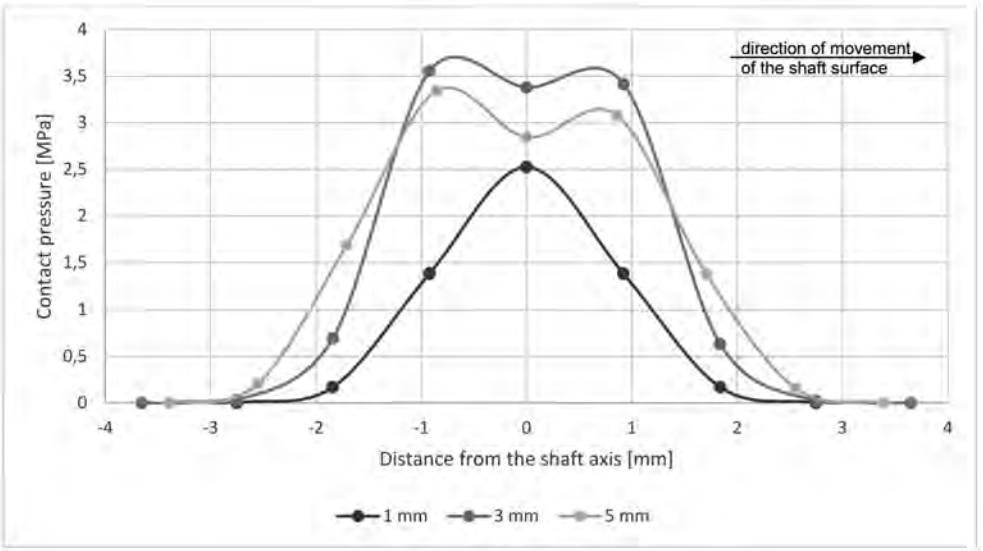


**Fig. 10. Distribution of the contact pressure between the shaft and the pan for PEEK at $T$ = 20°C for different thicknesses of the pan**

Rys. 10. Rozkład nacisków stykowych między wałem a panewką dla PEEK w temperaturze $T$ = -20°C dla różnych grubości panewki

## REFERENCES

1. Chang, L.; Zhang, Z.; Ye, L.; Friedrich, K.: Tribological properties of high temperature resistant polymer composites with fine particles. Tribol. Int. 2007, 40, pp. 1170–1178, doi:10.1016/j.triboint.2006.12.002.
2. Kurdi, A.; Kan, W.H.; Chang, L.: Tribological behaviour of high performance polymers and polymer composites at elevated temperature. Tribol. Int. 2019, pp. 130, 94–105, doi:10.1016/j.triboint.2018.09.010.
3. Pawelec, Z.; Dasiewicz, J.: Charakterystyki tribologiczne skojarzenia kompozyt polimerowy–brąz w podwyższonej temperaturze. Tribologia 2006, pp. 131–140.

4. Semenov, A.P.: Tribology at high temperatures. Tribol. Int. 1995, pp. 28, 45–50, doi:10.1016/0301-679X(95)99493-5.
5. Wan, S.; Tieu, A.K.; Xia, Y.; Zhu, H.; Tran, B.H.; Cui, S. An overview of inorganic polymer as potential lubricant additive for high temperature tribology. Tribol. Int. 2016, 102, pp. 620–635, doi:10.1016/j.triboint.2016.06.010.
6. Wang, Y.; Chen, W.: Microstructures, properties and high-temperature carburization resistances of HVOF thermal sprayed NiAl intermetallic-based alloy coatings. Surf. Coatings Technol. 2004, 183, pp. 18–28, doi:10.1016/j.surfcoat.2003.08.080.
7. Yano, O.; Yamaoka, H.: Cryogenic properties of polymers. Prog. Polym. Sci. 1995, 20, pp. 585–613, doi:10.1016/0079-6700(95)00003-X.
8. Zhang, Y.H.; Wu, J.T.; Fu, S.Y.; Yang, S.Y.; Li, Y.; Fan, L.; Li, R.K.Y.; Li, L.F.; Yan, Q.: Studies on characterization and cryogenic mechanical properties of polyimide-layered silicate nanocomposite films. Polymer (Guildf). 2004, 45, pp. 7579–7587, doi:10.1016/j.polymer.2004.08.032.
9. Indumathi, J.; Bijwe, J.; Ghosh, A.K.; Fahim, M.; Krishnaraj, N.: Wear of cryo-treated engineering polymers and composites. Wear 1999, pp. 225–229, 343–353, doi:10.1016/S0043-1648(99)00063-0.
10. Theiler, G.: PTFE- and PEEK – Matrix Composites for Tribological Applications at Cryogenic Temperatures and in Hydrogen; 2005.
11. Ptak, A.; Kowalewski, P.: The Influence of Reducing Temperature on Changing Young'S Modulus and the Coefficient of Friction of Selected Sliding Polymers. Tribologia 2018, 279, pp. 107–111, doi:10.5604/01.3001.0012.7018.
12. Chu, X.X.; Wu, Z.X.; Huang, R.J.; Zhou, Y.; Li, L.F.: Mechanical and thermal expansion properties of glass fibers reinforced PEEK composites at cryogenic temperatures. Elsevier, 2010.
13. Michael, P.C.; Rabinowicz, E.; Iwasa, Y.: Friction and wear of polymeric materials at 293, 77 and 4.2 K. Cryogenics (Guildf). 1991, pp. 31, 695–704, doi:10.1016/0011-2275(91)90230-T.
14. Gradt, T.; Schneider, T.; Hübner, W.; Börner, H.: Friction and wear at low temperatures. Int. J. Hydrogen Energy 1998, 23, pp. 397–403, doi:10.1016/s0360-3199(97)00070-0.
15. Gradt, T.; Börner, H.; Schneider, T.: Low temperature tribometers and the behaviour of ADLC coatings in cryogenic environment. Tribol. Int. 2001, 4, pp. 225–230.
16. Hübner, W.; Gradt, T.; Schneider, T.; Börner, H.: Tribological behaviour of materials at cryogenic temperatures. Wear 1998, 216, pp. 150–159, doi:10.1016/S0043-1648(97)00187-7.
17. Ptak, A.: Effect of loading time on the static friction polymer-metal sliding pairs at low temperature. In Proceedings of the Engineering Mechanics 2018; 2018; pp. 693–696.
18. Ptak, A.: The influence of the motion parameters on the surface layer of metal-polymer sliding pairs at low temperatures. Tribologia 2016, 265, pp. 79–87, doi:10.5604/01.3001.0010.7584.
19. Rusiński, E.; Czmochowski, J.; Smolnicki, T.: Zaawansowana metoda elementów skończonych w konstrukcjach nośnych; Oficyna Wydawnicza Politechniki Wrocławskiej, 2000.
20. Wieleba, W.: Bezobsługowe łożyska ślizgowe z polimerów termoplastycznych; Oficyna Wydawnicza Politechniki Wrocławskiej: Wrocław 2013.
21. Abo-Elkhier, M.: Elasto-plastic finite element modelling of strip cold rolling using Eulerian fixed mesh technique. Finite Elem. Anal. Des. 1997, 27, pp. 323–334.
22. Bijak-Zochowski, M.; Marek, P.: Residual stress in some elasto-plastic problems of rolling contact with friction. Int. J. Mech. Sci. 1997, doi:10.1016/0020-7403(96)00018-5.
23. Barbour, P.S.M.; Barton, D.C.; Fisher, J.: The influence of stress conditions on the wear of UHMWPE for total joint replacements. J. Mater. Sci. Mater. Med. 1997, 8, pp. 603–611, doi:10.1023/A:1018515318630.
24. Kowalewski, P.: Numeryczna analiza rozkładów nacisku występujących w standardowych węzłach tribologicznych. Tribologia 2010, 39, pp. 39–47.
25. Smolnicki, T.: Wielkogabarytowe toczne węzły obrotowe: zagadnienia globalne i lokalne; 2013.
26. Biernacki, K.: Estimation of the Coefficient of Static Friction By Means of Numerical Analysis. Tribologia 2019, 287, pp. 19–24, doi:10.5604/01.3001.0013.6557.
27. Du, S.; Hamdi, M.; Sue, H.J.: Experimental and FEM analysis of mar behavior on amorphous polymers. Wear 2020, 444–445, 203155, doi:10.1016/j.wear.2019.203155.
28. Wieleba, W.: Modelowanie procesów tribologicznych z wykorzystaniem techniki komputerowej. Górnictwo Odkryw. 2010, 3, pp. 224–227.
29. Kowalewski, P.: Modelowanie tarcia w endoprotezie stawu kolanowego, Politechnika Wrocławska, 2007.
30. Wieleba, W.: Metoda numeryczno-doświadczalna wyznaczania oporów tarcia w polimerowych łożyskach ślizgowych podczas rozruchu. Tribologia 2007, 3, pp. 329–337.
31. Ptak, A.: Mechanizmy tarcia wybranych polimerów termoplastycznych po stali w niskiej temperaturze, 2014.
32. Kowalewski, P.: Tarcie polimerów termoplastycznych w warunkach złożonego ruchu. 2019.